CORPUS CALLOSAL MICROSTRUCTURE PREDICTS BIMANUAL MOTOR PERFORMANCE IN CHRONIC STROKE SURVIVORS

Rini Varghese, MS
Brianna Chang, BS
Bokkyu Kim, PhD, PT
Sook-Lei Liew, PhD, OTR/L
Nicolas Schweighofer, PhD
Carolee J. Winstein, PhD, PT

ABSTRACT

Much of the research using diffusion tensor imaging (DTI) in stroke focuses on characterizing the microstructural status of corticospinal tracts and its utility as a prognostic biomarker. However, the ischemic event in the lesioned cortex also triggers structural and functional alterations in its contralateral homolog through the corpus callosum (CC), known as transcallosal diaschisis. The few studies that have characterized the microstructural status of the CC using DTI only examine its relationship with paretic limb performance. Given the well-established role of the CC for bimanual coordination, especially fibers connecting the larger sensorimotor networks such as prefrontal, premotor and supplementary motor regions, we examine the relationship between the microstructural status of the CC and bimanual performance in chronic stroke survivors (n = 41). We used movement times for two self-initiated and self-paced bimanual tasks to capture bimanual performance. Using publicly available control datasets (n = 52), matched closely for acquisition parameters, including sequence, diffusion gradient strength and number of directions, we also explored the effect of age and stroke on callosal microstructure. We found that callosal microstructure was significantly associated with bimanual performance in chronic stroke survivors such that those with lower callosal FA were slower at completing the bimanual task. Notably, while the primary sensorimotor regions (CC3) showed the strongest relationship with bimanual performance, this was closely followed by the premotor/supplementary motor (CC2) and the prefrontal (CC1) regions. We used multiple mixed regression to systematically account for loss of callosal axons (i.e., normalized callosal volume) as well as differences in lesion size and other metrics of structural damage. Chronic stroke survivors presented with significantly greater loss of callosal fiber orientation (lower mean FA) compared to neurologically intact, age-similar controls, who in turn presented with lower callosal FA compared to younger controls. The effect of age and stroke were observed for all regions of the CC except the splenium. These preliminary findings suggest that in chronic stroke survivors with relatively localized lesions, callosal microstructure can be expected to change beyond the primary sensorimotor regions and might impact coordinated performance of self-initiated and cooperative bimanual tasks.

Keywords: diffusion tensor imaging, stroke, corpus callosum, bimanual, recovery, behavior

1. INTRODUCTION

Focal ischemic injury to the central nervous system can result in changes remote from the site of injury (*diaschisis,* von Monakow, 1914). One such case is *transcallosal* diaschisis in which the ischemic event in the lesioned cortex triggers structural and functional alterations in its contralateral homolog through the corpus callosum. Although the exact mechanism of transhemispheric diaschisis in humans is not well understood, evidence from animal models suggests a dual process (Jones & Adkins, 2015). First, early after the injury, diaschisis is evidenced by reductions in cellular metabolism and local cerebral perfusion in the ischemic penumbra. As a result, axon terminals of transcallosal afferents originating from the lesion site degenerate and cause higher-order axons to systematically eliminate or prune away from the intact cortex. In behaviorally adaptive animals, this is simultaneously accompanied by a second process of reactive synaptogenesis and dendritic arborization in the intact cortex, secondary to the nonuse of the weak limb and compensatory overuse of the healthy limb. The severity of asymmetry in limb use is directly related to the size of the arbors, which over time, with the recovery of symmetric limb use, are pruned (Jones & Schallert, 1994).

The reactive growth and reorganization process in the intact hemisphere stabilizes in the subacute and chronic phases (Jones & Schallert, 1992) and provides unique insight into post-stroke recovery. Because reinnervation is accomplished during this time through the sprouting of collaterals from existing axons rather than the genesis of new long-distance neurons, this process is most likely to alter the microstructure and connectivity of local axon pools within a given region. In humans, such microstructural changes can be noninvasively approximated using diffusion tensor imaging (DTI).

There is growing evidence for the utility of DTI-derived metrics in humans as prognostic biomarkers of recovery after stroke (Kim & Winstein, 2017; Puig et al., 2017). Microstructural status of the corticospinal tract, principally the composite fractional anisotropy measure (FA), has been shown to predict short and long-term outcomes including stroke severity, disability, functional improvement (Kim, 2017; Lindenberg et al., 2012), and sensorimotor performance (Findlater et al., 2019) in chronic stroke.

In recent years, DTI has also revealed interesting patterns of transcallosal diaschisis and reorganization in humans (Egorova et al., 2020; Hawe et al., 2013; Yeh et al., 2013) and its association with functional motor recovery. For example, compared to controls, lower FA values in the corpus callosum (CC) have been observed in the subacute (Li et al., 2015; Wang et al., 2012) and chronic phase after stroke (Stewart, Dewanjee, et al., 2017; Stewart, O'Donnell, et al., 2017). In the latter study, lower FA in the motor region of the CC was found to correlate with greater sensorimotor impairment in the paretic hand. In chronic stroke survivors, microstructural status of the CC also predicted response to therapy. Specifically, lower FA in the motor CC at baseline was negatively correlated with change in motor function following treatment with a combined intervention consisting of tDCS with physical/ occupational therapy (Lindenberg et al., 2012). However, the aforementioned studies were limited by small sample sizes, an almost exclusive focus on the primary sensorimotor regions of the CC, and traditional clinical measures of paretic hand motor impairment, which might not directly correspond to changes in CC microstructure.

To address these limitations, the primary purpose of this study was to determine if CC microstructure predicts bimanual motor performance in chronic stroke survivors, looking in a

larger sample of 41 chronic stroke survivors and examining all regions of the CC. We utilized a bimanual task because we expected that the chronic persistence of lower FA in the non-sensorimotor regions of CC might be detrimental to motor performance not captured by traditional clinical measures of paretic hand motor impairment, which are thought to have plateaued in the chronic phase (Krakauer & Carmichael, 2017). In particular, motor outcomes assessed in the previous studies of CC were singularly focused on the paretic limb, e.g., impairment (UEFM, Li et al., 2015; Stewart, Dewanjee, et al., 2017; Wang et al., 2012), self-reported disability (NDS, SIS hand, Li et al., 2015; Stewart, Dewanjee, et al., 2017), and function (WMFT, Lindenberg et al., 2012, ARAT, Li et al., 2015). However, based on the long-established evidence for the role of CC in interlimb coordination (Bonzano et al., 2008; Caeyenberghs et al., 2011; B. W. Fling & Seidler, 2012; Brett W. Fling et al., 2011; Franz et al., 1996; Gooijers et al., 2013; Sisti et al., 2012), one might expect that the lower FA in non-sensorimotor callosal regions might be better reflected in the performance of tasks that preferentially engage bi-hemispheric circuits, such as bimanual tasks. As noted earlier, studies in rodent models of stroke suggest that the reactive synaptogenesis and reorganization in the intact hemisphere did not simply emerge in response to repetitive motor activity of the healthy limb, but rather required a skill learning process. Therefore, successful compensatory behaviors learned over time may contribute to the transcallosal reorganization process and we expect would be associated with the microstructural status of the non-sensorimotor regions of CC. To capture performance on such use-dependent, learned motor behaviors, we unobtrusively observed natural arm use for two components of a bimanual task (folding and inserting a letter into an envelope) and quantified the time taken to complete this task.

In addition to studying this task performance in relation to the sensorimotor region of the CC, we also examined non-sensorimotor regions of CC. Two candidates of special interest for the control of bimanual skills based on previous evidence were the prefrontal region (CC1) involved in higher-order planning and response selection (Baxter et al., 2000; Rowe et al., 2000), and, the premotor and supplementary motor regions (CC2), involved in temporal sequencing (Halsband et al., 1993; Kornysheva & Diedrichsen, 2014; Sadato et al., 1997). We hypothesized that lower FA in not only the primary sensorimotor but also CC1 and CC2, would correspond with poor performance on the bimanual task.

Finally, considering that following a stroke, there are widespread alterations in bilateral brain excitability and brain health (Egorova et al., 2019; Gratton et al., 2012), it is plausible that the callosal microstructure is also affected in regions directly neighboring the sensorimotor cortices, such as CC2 and CC5. Some support for this hypothesis comes from a study by Hayward and colleagues in which they found that in chronic stroke survivors, FA of the anterior regions of the CC, specifically fibers connecting the prefrontal cortices, was positively correlated with paretic hand motor impairment (Hayward et al., 2017). Although it does not directly neighbor the primary motor cortex, the authors argued that the microstructure of the prefrontal cortex could influence motor impairment via indirect connections through the premotor area. Recently, similar to the study by Hayward and colleagues, Pinter et al., 2020 reported that lower FA in the callosal genu, which corresponds to the fibers connecting the prefrontal areas, recorded within 72 hours after stroke (acute phase) along with a general disability measure (modified Rankin scale) explained 53.5% of the variance in stroke recovery at 3 months. In the same study, the authors also noted that compared to a control group, FA was lower for *all* regions of the CC. Although a control group was not examined in the Hayward study, we hypothesized that FA reductions across the CC, especially in the non-

sensorimotor regions, as reported by Pinter, may persist in the chronic phase. Here, we performed a secondary exploratory analysis to examine this idea. Using both our own data and publicly available data, we compared FA reductions in chronic stroke survivors that we collected with that of neurologically intact controls from a publicly available dataset. The control dataset allowed us to more cleanly isolate the effects of stroke from the more general effects of age, establishing a baseline from which the stroke effects can be compared. Based on Pinter et al and Hayward et al., we hypothesized that compared to age-similar controls, FA would be significantly reduced, beyond the general reductions from aging, in all regions of the CC, including the non-sensorimotor regions.

2. METHODS

2.1. Participants

Diffusion tensor imaging data for 41 chronic stroke survivors were available from a Phase 2B randomized controlled trial (Dose Optimization for Stroke Evaluation, ClinicalTrials.gov ID: NCT01749358) (Winstein et al., 2019). Only baseline data from the DOSE study were included in this analysis. These data were collected between 2012 and 2015 on the Health Sciences Campus of the University of Southern California (USC).

For our exploratory analysis examining differences in the microstructural status of the CC in chronic stroke survivors versus healthy controls, we used publicly available diffusion datasets acquired in 24 age-similar older adults and 28 younger adults, matched closely for acquisition parameters, including sequence, diffusion gradient strength and number of directions (OpenNeuro.org ID: ds001242). These data were collected between 2016 and 2018 on the University Park Campus of USC.

All individuals gave informed consent to participate in the two studies in accordance with the 1964 Declaration of Helsinki and the guidelines of the Institutional Review Boards of the respective campuses of USC where the data were collected.

2.2. Diffusion Imaging

2.2.1. Acquisition

The diffusion MRI scans in stroke survivors was acquired on a GE Signa Excite 3T scanner using a single shot spin echo EPI pulse sequence with the following parameters: TR = 10,000 ms, TE = 88 ms, FoV = 256 mm, 75 axial slices of thickness = 2.0 mm, gradient strength of 1000s/mm^2 in 64 diffusion gradient directions. This generated a 2 x 2 x 2 voxel size and a matrix size of 128 x 128. A high-resolution structural T1-weighted image was acquired prior to diffusion imaging using the gradient-echo (SPGR) sequence with the following parameters: TR = 24 ms, TE = 3.5 ms, flip angle = 20˚, FoV = 240 mm, and slice thickness = 1.2 mm with no gaps, generating a matrix size of 197 x 233 x 189. Total time was approximately 20 minutes.

The younger and age-similar older control datasets were acquired on a Siemens 3T Trio Total imaging matrix (Tim) system. A comparison of all scanner acquisition parameters is provided in the Supplementary Material (I).

2.2.2. Preprocessing

Data pre-processing and analysis followed a standard pipeline using the FMRI Software Library, FSL (Figure 1). Voxel-wise statistical analysis of the FA data was carried out using TBSS (Tract-Based Spatial Statistics, Smith et al., 2006), part of FSL (Smith et al., 2004). Diffusion

images were first preprocessed, including correction for eddy currents and motion-related distortion, followed by brain extraction (BET2, Jenkinson et al., 2005). Next, FA images were created by fitting a tensor model to the preprocessed diffusion data using FDT (Smith, 2002). All subjects' FA data were then aligned into a common space (FMRIB58_FA) using the nonlinear registration tool FNIRT (Andersson et al., 2007a, 2007b), which uses a b-spline representation of the registration warp field (Rueckert et al., 1999). The FMRIB58_FA is a white matter template generated from an average of 58 high-resolution, well-aligned FA images from healthy adults and is in the same coordinate space as the 1mm MNI 152 template. Visual quality checks (QC) were performed at every step and manual adjustments were made as necessary. Lastly, the mean FA image was created and thinned to render an FA skeleton which represents the centers of all tracts common to the group. Each subject's aligned FA data was then projected onto this skeleton and a voxel-wise threshold FA of 0.2 is applied to remove any edge effects.

--- Figure 1 ---

Figure 1. a) Diffusion pipeline including preprocessing, co-registration and identifying region of interest (i.e., corpus callosum). (b) Parcellation (from posterior to anterior) of the corpus callosum using the geometric scheme proposed by Hofer & Frahm (2006). (c) Table showing cortical regions connected by the fibers running through each of the five CC parcels.

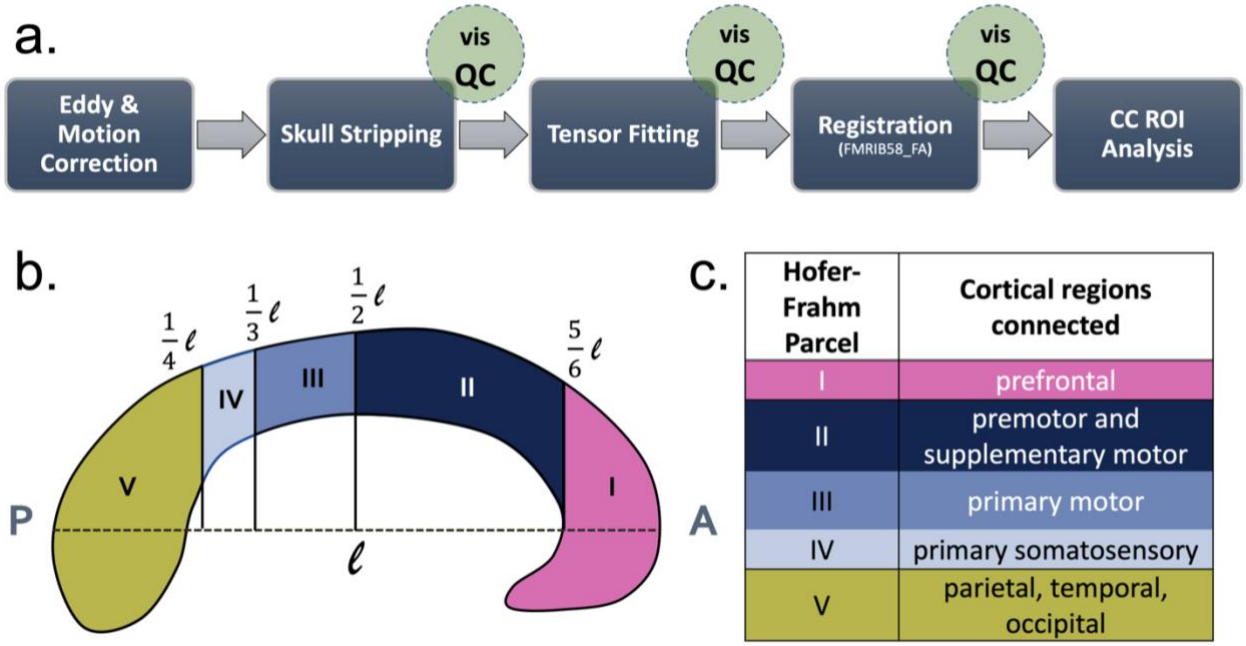

Hofer-Frahm Parcel	Cortical regions connected
I	prefrontal
II	premotor and supplementary motor
III	primary motor
IV	primary somatosensory
V	parietal, temporal, occipital

2.3. Assessment of Callosal Microstructure

The corpus callosum (CC) was defined as the primary region of interest. To assess microstructural status of the CC, we analyzed diffusion images in the standard space, and used the JHU white matter atlas to mask the CC (JHU ICBM-DTI-81 White-Matter Labels). The CC was then segmented geometrically on the midsagittal plane into five subregions according to the Hofer-Frahm parcellation scheme (Hofer & Frahm, 2006). Each of these segments correspond to fibers connecting homotopic regions of the prefrontal (I), premotor and supplementary motor (II), primary motor (III), primary somatosensory (IV), and parietal, temporo-occipital (V) cortices, which in the standard MNI space, consists of 8851, 6871, 5803, 2619, 12729 voxels respectively. Mask templates are available in the first author's OSF repository: osf.io/7j9xe

Microstructural status was quantified as the fractional anisotropy (FA) index. The FA index is a composite measure reflecting the 3-dimensional directional characteristics of diffusion in each voxel, serving as a proxy for fiber orientation (Hagmann et al., 2006; Pierpaoli & Basser, 1996; Soares et al., 2013). It is computed as a normalized fraction of the eigenvalues derived directly from voxel-wise fitted tensors, and ranges from 0 (isotropic diffusion, spherical in shape) to 1 (anisotropic diffusion, ellipsoidal in shape). The FA composite measure works particularly well for directionally homogenous, well-aligned fibers such as those of the CC, especially after thresholding for edge effects. In a random subset of stroke survivors (n = 20), we validated the FA index generated in the standard-space CC mask with those in the native FA maps and found no difference in mean FA between the two spaces. Results from these comparisons and related bootstrap analyses are provided in Supplementary Materials (II).

In stroke survivors only, we also computed tissue volume as an index of CC macrostructure. To do this, individual CC masks were drawn in the native space of each participant's structural T1 image using ITK-SNAP (v. 3.8). We normalized CC volumes to express them as a percentage of total white matter volume. To compute total white matter volume, we performed tissue segmentation using FSL's FAST routine with visual quality checking to ensure that all of the viable white matter tissue, sparing the lesion, was identified in the segmentation procedure.

2.4. Lesion Reconstruction

Stroke lesions were manually drawn on structural T1 images by trained personnel using MRIcron, an open-source tool for segmentation and visualization (Rorden & Brett, 2000). A detailed procedure has been described previously and all T1-weighted images and binarized lesion masks are available as part of the ATLAS stroke lesion database, vR1.1 (Liew et al., 2017). Lesion volume was calculated using FSL's *fslstats* function. A lesion overlap image among stroke survivors was generated using the *fslmaths -add* function and visualized in FSLeyes (Jenkinson et al., 2012). Figure 2 shows lesion overlap among 41 chronic stroke survivors.

--- Figure 2 ---

Figure 2. Overlap of lesions for 41 chronic stroke survivors. Note that images were not flipped and represent the actual side of unilateral stroke.

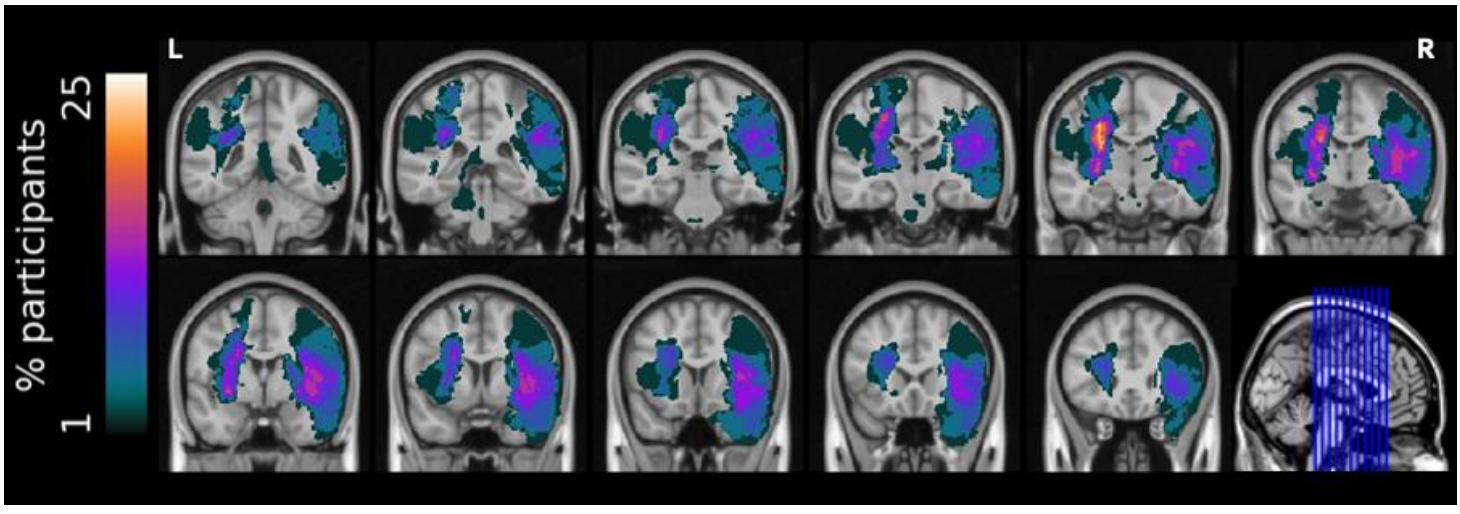

2.5. Bimanual Motor Performance

In conjunction with diffusion imaging, behavioral data for 33 of the 41 right-handed stroke survivors were available for analysis. The behavioral paradigm has been described in detail previously (Varghese et al., 2020). Briefly, participants were covertly observed as they performed a natural bimanual task—the letter-envelope task—of the Actual Amount of Use Test. Data were captured on video and analyzed offline to quantify whether participants chose one or both hands and the time taken to complete the task at self-selected speed, i.e., movement time.

The letter-envelope task consisted of two components: folding the letter followed closely by inserting the letter into the envelope. Start times were defined as the frame when initial contact was made with the letter or envelope, and end times were defined as the frame when the goal was accomplished, i.e., when the last fold was completed, or letter was fully inserted into the envelope. Movement time (MT) was defined as the time elapsed between the start and end time points and was determined for each component of the composite task. For the current analysis, we analyzed MTs for those participants who chose a bimanual strategy.

We selected the letter-envelope task because a majority of the participants (31 out of 33) chose a bimanual strategy for at least one of its components (see Supplementary Material II). However, not every participant performed both components of the task bimanually. Regardless, MT for every one of the 31 participants who chose a bimanual strategy were included in the statistical analysis and allowed us to maintain as complete a set of matched brain imaging and behavioral data as was possible.

Given that the strategy was self-selected, the speed was self-paced, and the testing itself was conducted unbeknownst to the participants, performance on this task was largely unconstrained, and served as a proxy for interlimb coordination as if it were in the real world, even if qualitatively variable for each individual. In other words, it served as a reasonable representation of well-learned stereotypical arm use behaviors that stroke survivors may have deemed useful for successfully accomplishing every day bimanual tasks.

2.6. Statistical Analysis

All analyses were conducted using the R statistical computing package (version 3.5.1). All continuous variables, age, chronicity, Upper Extremity Fugl-Meyer scores (UEFM), and movement time, were assessed for normality. Distributions for chronicity and movement time were positively skewed and so they were log-transformed. Assumptions for generalized linear models, including linearity, equality of variance, independence and normality of errors were met and model diagnostics, including leverage and multicollinearity of independent variables, were tested when appropriate.

2.6.1. Relationship between callosal microstructure and bimanual behavior in chronic stroke survivors

First, in chronic stroke survivors only, to determine the relationship between mean callosal FA and bimanual MT, we used robust linear mixed effects regression of the form below:

A robust model was used instead of a simple linear mixed-effects (LMER) approach because diagnostics revealed 1 participant whose MT had a very low value (2.8 seconds) which

was 1.77 SD away from and Cook's distance of 0.03. As this point deviated substantially from the rest of the participants, but its Cook's distance was not so large as to warrant its removal, we preserved it in our sample pool and used robust linear mixed effects. We suspected high multicollinearity between the CC regions but found a somewhat small variance inflation factor of 1.14.

$$log(MT) \sim Mean\ FA + Mean\ FA{:}\ CC\ region + log(Chronicity) + CC\ volume + (1|CC\ region{:}\ subject) \quad \ldots(1)$$

In the above model, mean FA was the average FA across all voxels in a given region of the CC. CC region was a dummy categorical variable with 5 levels, each to code for the 5 segments of the CC, with CC3 (motor) set as the reference level. We hypothesized that mean FA would be significantly different from 0 for CC3 (primary motor) and CC4 (primary sensory), but also for CC1 (prefrontal) and CC2 (premotor/supplementary motor). We tested this using individual post-hoc t-tests of the estimated marginal trends. We also suspected that the slope of this relationship might be moderated by CC region, so we included an interaction term to test this. Pairwise comparisons of slopes for each CC region were conducted using Tukey's HSD. Finally, because a single value for MT per subject was repeated over five CC regions, there was no reason to suspect MT to change over the levels of CC region. Instead, to estimate this additive shift arising from subject- and CC region-wise differences in intercepts, we modeled the random effects as an interaction between subject and CC region. By so doing, we were able to estimate variances from the additive shifts for both subject and CC region: for instance, mean FA value for CC5 could be higher than CC3 in subj#1 but lower in subj#5.

We arrived at the final model (eq. 1) by using a combined—forward then backwards stepwise approach, in which we tested for the confounding effects of age, sex, chronicity, side of lesion, UEFM score, and normalized total CC volume by adding them to the base model that consisted only of mean FA and CC region. We preserved any covariate that met a cut-off of $p = 0.1$ in a combined model. Then, from the combined model, we removed predictors that were not significant ($p < 0.05$). Based on this selection process, only log-transformed chronicity and normalized total CC volume were included in the above final model. Notably, by including normalized total CC volume, we were able to take into account the likely loss in CC tissue volume.

Lastly, to further corroborate our analysis, we asked whether traditional metrics of unilateral structural damage provided any additional explanatory power to our final model above. We did so by adding five measures of corticospinal tract integrity, lesion, and brain atrophy (Kim, 2017; Liew et al., 2017): 1) CST FA asymmetry index, 2) CST lesion load, 3) lesion volume, 4) lesion FA, and 5) ventricular volume asymmetry. All metrics, except lesion volume, were computed previously by one of the authors (BK), and available for 29 of the 31 participants for whom bimanual MT data were also available. As a result of unequal sample sizes however, models could only be compared using marginal R^2.

2.6.2. Comparing callosal microstructure between chronic stroke survivors and neurologically intact adults

Second, to explore the effect of stroke on mean callosal FA, we used linear mixed effects regression of the following form:

$$Mean\ FA \sim Group\ +\ CC\ region\ +\ Group:\ CC\ region\ +\ (1|subj)\ +\ (1|scanner:subj)\ \ldots(2)$$

Pairwise comparisons of estimated marginal means for each CC region were conducted using Tukey's HSD. Our hypothesis was that mean FA would be lower in stroke survivors compared to age-similar adults. We suspected that while group effects would be largest for CC3 (motor) directly adjacent regions (e.g., CC2, premotor) would also show significant reductions in FA. Given that our data were obtained from two different scanners, random effects were estimated as random intercepts for both subject- and scanner-related variances.

Here again, we arrived at the final model (eq. 2) through the same process described above, testing for the confounding effects of age and sex; neither met a cut-off $p = 0.1$, so were removed from the above final model. Note that age was in fact partially embedded within the grouping factor itself. However, because testing for age-related effects on FA was not the primary purpose of this study, we only preserved age as a categorical variable. A supplementary analysis of the relationship between age and FA is provided for the interested reader (Supplementary Material IV).

A one-way ANOVA was used to compare age among the three groups (i.e., younger controls, older controls, and stroke survivors) followed by pairwise comparisons using Tukey's HSD. Kruskal-Wallis test was used to compare the proportion of females and males among the three groups. Significance was set at p = 0.05 and adjusted for multiple comparisons when necessary.

3. RESULTS

Of the 93 adults whose data were analyzed for this study, 41 were chronic stroke survivors, and 52 were neurologically intact. The average age was 50.7 years and there were 64 males (68.8%) (see Table 1 for full details). Of the controls, 24 were older adults and 28 were younger adults. There was a significant difference in age between the young controls and the two older groups (F (2,90) = 156.73, $p < 0.001$)—older controls (Δ age = 43 years) and stroke survivors (Δ age = 35 years). The stroke group was also younger than the age-similar control group (Δ age = 8 years). There was a similar representation of sex among the three groups (H (2) = 0.81, $p = 0.66$).

Within chronic stroke survivors, median chronicity was 1.9 years (IQR = 1.2–5.2) post stroke and median score on the upper extremity Fugl-Meyer (UEFM) was 43 (IQR = 31–50), indicating moderate impairment. Chronic stroke survivors consisted of 22 individuals with left hemisphere stroke and 19 with right hemisphere stroke. There was no significant difference in age ($p = 0.196$), sex ($p = 529$), chronicity ($p = 0.409$), or UEFM ($p = 0.633$) between the two stroke groups. Lesion volume was slightly larger in those with right hemisphere strokes but not significant (Δ mean = 1945.4 cc, $p = 0.054$). Table 1 provides demographic information.

On average across all stroke survivors, the lesion constituted < 0.05% (~11 voxels) of the total CC volume, whereas voxels of the CC constituted < 0.2% (~2 voxels) of the total lesion volume, confirming a very minor degree of direct injury to the CC (Figure 2). Individual descriptions of lesion locations are provided in the Supplementary Material (III).

--- Table 1 ---

Table 1. Subject characteristics.

	CONTROLS		
	Younger (N=28)	**Older (N=24)**	**STROKE (N=41)**
Age (years)			
Mean (SD)	24.4 (5.07)	67.0 (5.55)	59.1 (13.1)
Sex			
Female	9 (32.1%)	9 (37.5%)	11 (26.8%)
Male	19 (67.9%)	15 (62.5%)	30 (73.2%)
Chronicity (years)			
Median [Min, Max]			1.90 [0.474, 14.4]
UE Fugl-Meyer (/66)			
Median [Min, Max]			43.0 [19.0, 58.0]
Lesion Volume (cc)			
Median [Min, Max]			6.05 [0.0160, 121]

3.1. Lower callosal FA is associated with slower bimanual performance in chronic stroke survivors.

After accounting for chronicity and total normalized CC volume, mean FA in all regions of CC significantly predicted bimanual movement time in chronic stroke survivors, such that lower (more isotropic) FA was associated with slower performance. To interpret values in Table 2, please note again that CC3 was the reference level (thus Mean FA in Table 2 is the slope for CC3 and estimates for other levels are added to this estimate as described in the post-hoc marginal trends).

Post-hoc tests of marginal trends revealed that compared to 0, slope was largest for CC3 (motor, b = -4.01 ± 0.87, p < 0.001), followed closely by CC2 (premotor, b = -3.85 ± 0.84, p < 0.001) and CC1 (prefrontal, b = -3.65 ± 0.79, p < 0.001). In fact, the slope for CC3 did not significantly differ from CC1 and CC2 as observed in the interaction terms, Mean FA x CC1 and Mean FA x CC2. This suggests that consistent with our hypothesis, FA of premotor and prefrontal CC were both as predictive of bimanual MT as the motor CC. The slopes, however, were less steep for CC4 (sensory, b = -3.57 ± 0.78, p < 0.001) and CC5 (parietal, temporo-occipital, b = -3.22 ± 0.70, p < 0.001) as observed in the interaction terms, Mean FA x CC4 and Mean FA x CC5. However, post-hoc comparisons of all slopes revealed that the slope of only CC5 was significantly smaller than CC3 (t = -3.64, p = 0.003) and CC2 (t = -3.27, p = 0.012).

Table 2 provides model estimates from robust regression and Figure 3 illustrates the relationship using model fitted predictions.

--- Table 2 ---

Table 2. Robust mixed-effects regression coefficients from Model (1) to estimate relationship between bimanual movement time and mean fractional anisotropy (FA) for five segmented regions of the CC relative to the reference group (CC3, motor).

		log(mt)	
Predictors	*Estimates*	*CI*	*p*
Intercept	5.59	4.49 – 6.69	**<0.001**
Mean FA	-4.01	-5.72 – -2.30	**<0.001**
log(Chronicity)	0.15	0.07 – 0.24	**<0.001**
Total Normalized CC Volume	-0.19	-0.33 – -0.04	**0.011**
Mean FA x CC1	0.36	-0.01 – 0.73	0.057
Mean FA x CC2	0.16	-0.20 – 0.51	0.386
Mean FA x CC4	0.43	0.05 – 0.81	**0.025**
Mean FA x CC5	0.78	0.33 – 1.24	**0.001**
Random Effects			
σ^2	0.17		
$\tau_{00\ CC\_region:subjID}$	0.11		
ICC	0.39		
N_{CC_region}	5		
N_{subjID}	31		
Observations	270		
Marginal R^2 / Conditional R^2	0.204 / 0.514		

Finally, by individually including traditional measures of structural damage in our model, we found that of the five CST and lesion metrics, three contributed a statistically significant additive value to CC FA in predicting bimanual movement time: ventricular volume asymmetry, CST lesion load, and lesion FA. When combined together in the same model, marginal R^2 improved by 16.9%, from 20.4% to 37.3%; however, only lesion FA (t = -3.87, p < 0.001) and ventricular volume asymmetry (t = 3.54, p < 0.001) remained significant. These results

suggest that in addition to callosal FA, lower FA in the white matter directly underlying the lesion and the relative enlargement of the ipsilesional lateral ventricle predicted slower bimanual performance. Model comparisons and model results with these two factors are provided in the Supplementary Material (V).

--- Figure 3 ---

Figure 3. Callosal FA for each of the five regions plotted against log-transformed movement times for the two bimanual tasks. Population regression lines from robust mixed effects regression are shown.

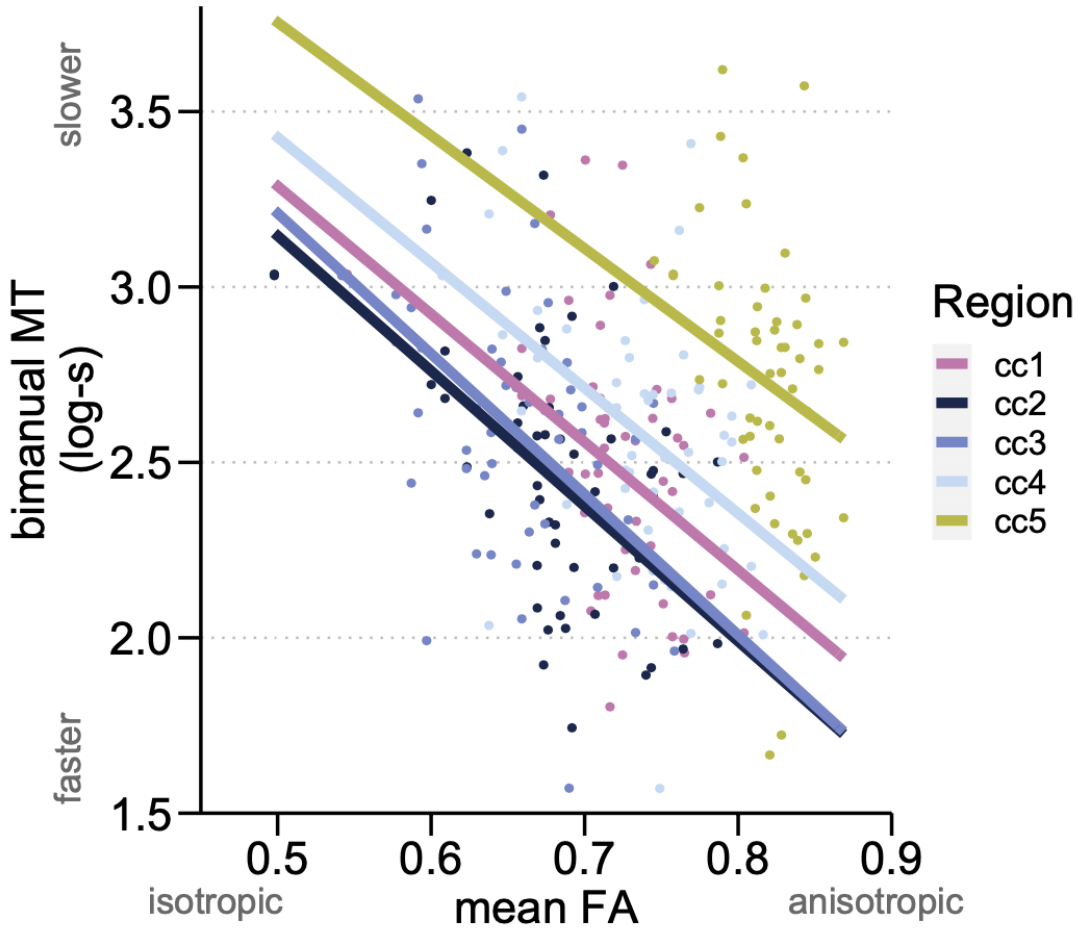

3.2. Compared to neurologically intact adults, chronic stroke survivors exhibit lower FA in all regions of the CC, except the splenium.

There was a significant interaction between group and CC region (F (8, 360) = 21.01, p < 0.001). Compared to neurologically intact older adults, mean FA was lower for all CC regions, except the splenium (parietal, temporo-occipital region). Greatest decrements were seen for the

primary motor region, CC3 (ΔFA = 0.052, t = 4.84, p < 0.001), but was closely followed by the premotor and supplementary motor, CC2 (ΔFA = 0.050, t = 4.69, p < 0.001), primary sensory, CC4 (ΔFA = 0.034, t = 3.15, p = 0.005), and lastly prefrontal regions, CC1 (ΔFA = 0.029, t = 2.73, p = 0.02). Figure 4 illustrates this interaction using model estimated marginal means.

--- Figure 4 ---

Figure 4. Model estimated marginal means for CC FA across the five regions along with individual data points. * p < 0.05, ** p < 0.01, *** p < 0.001.

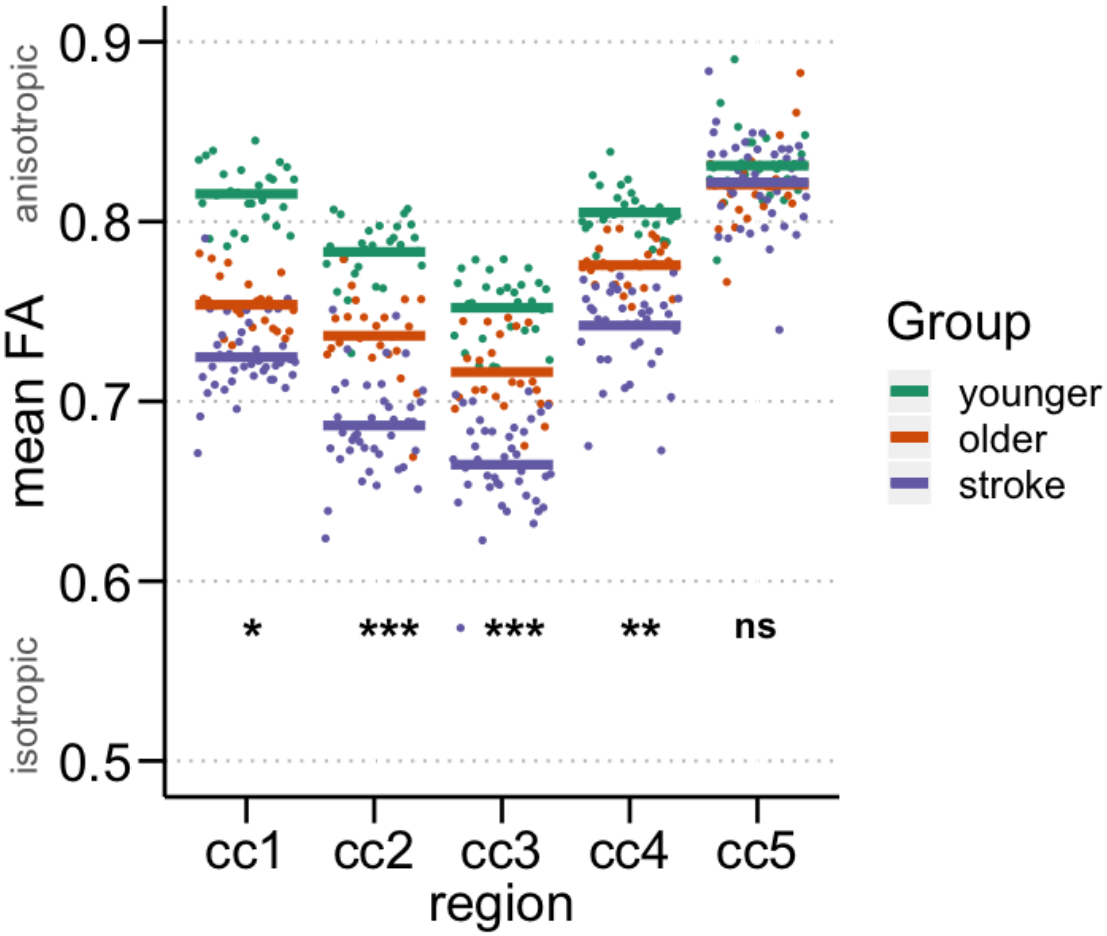

4. DISCUSSION

There were two main findings in this study: First, callosal microstructure was significantly associated with bimanual performance in chronic stroke survivors. Notably, a significant relationship was observed not only with the primary sensorimotor regions (CC3), but also regions of the premotor/supplementary motor (CC2) and prefrontal (CC1) regions. While previous studies have reported on the association of callosal microstructure with unimanual motor outcomes of performance, impairment, function, and general disability, this finding is, to our knowledge, the first demonstration of a relationship between bimanual performance and callosal microstructure in stroke survivors. Second, chronic stroke survivors presented with significantly greater loss of callosal fiber orientation (lower mean FA), compared to neurologically intact adults. This finding confirms and extends previous reports.

4.1. Primary motor, premotor and supplementary motor CC show strongest relationship with bimanual performance in chronic stroke survivors

After accounting for callosal volume and the time after stroke, lower mean FA across the CC was associated with longer movement times for a cooperative and sequential bimanual task. As expected, the largest slope between bimanual MT and FA was seen for the primary motor region of the CC (CC3), followed closely by the secondary motor regions (CC2). With stroke lesions largely localized to the motor subcortical areas and descending motor pathways, the involvement of the primary motor CC was not surprising. Microstructural changes in this region of the callosum may be closely linked to its evolving role in regulating premovement inhibition† especially in the chronic phase.

A novel demonstration in this study is the relationship between CC2, the rostral portion of the body of the CC that connects homotopic premotor and supplementary motor regions, and bimanual performance in stroke. The medial wall of the frontal lobe has been shown to be causally involved in the control of self-initiated, self-paced cooperative bimanual movements (Brinkman & Kuypers, 1973; Kazennikov et al., 1998; Preilowski, 1972; Stephan et al., 1999). Patients who had undergone anterior callosotomy were significantly slower and the timing of movement initiations with both limbs were more imprecise (Eliassen et al., 2000) than in controls. Preliowsky inferred that this may be because the anterior CC serves as a more direct route for the sharing of motor corollary discharges in the frontal lobe, enabling faster bimanual performance. The bimanual task we examined was cooperative, and participants were observed covertly as they self-initiated a movement strategy and completed the task at self-selected speed. Although not as extreme as callosotomy, it stands to reason that poor microstructural status of the anterior callosum in stroke survivors, delays transcallosal exchange of corollary discharges and slows bimanual performance on such a task.

The splenium (CC5) also showed a significant relationship with bimanual motor performance, but the slope of this relationship was significantly less steep compared to CC2 and CC3. Given that the task required processing of visual signals before and during

†One function of the callosal fibers in CC3 is to carry inhibitory signals between the motor cortices. This mutual inhibition, exerted especially in the pre-movement phase of unimanual movements, regulates undue excitability of the unengaged motor cortex and allows minimal interference in the outgoing command signal from the engaged one. A prevailing hypothesis to explain persistence of paretic limb impairment in the chronic phase after stroke is a failure to release premovement inhibition.

performance, it would make sense why lower FA of the posterior fibers of the CC correlates with slower movement times. However, because CC5 consists of a heterogeneous fiber population originating from the parietal, temporal and occipital regions, it is difficult to disambiguate if the associations with slower MT is due to deficits in primary visual processing or higher order sensory integration. It is important to note that the splenium itself was largely spared from the observed effects of stroke (more details in the next section), thus, the range of FA values observed (0.74-0.87) was smaller than that in the body (0.49-0.78) and the genu (0.54-0.80) of the CC. This may explain why the observed effects for CC5 were smaller than CC2 and CC3. Another explanation is that our measure of movement time did not capture features of performance that might better reflect functions of the posterior callosum, such as visuospatial integration and accuracy (Franz et al., 1996).

4.2. The effects of stroke on CC regions connecting the larger sensorimotor networks

Compared to neurologically intact controls, chronic stroke survivors showed significant reduction in FA across the genu (CC1) and body (CC 2, 3, 4) of the corpus callosum, but no difference was found in the splenium (CC5). We extended previous findings of lower callosal FA in acute stroke (Pinter et al., 2020) survivors to the chronic phase, in those with mild to moderate motor impairment (Hayward et al., 2017; Stewart, Dewanjee, et al., 2017), and in pediatric hemiplegia (Hawe et al., 2013). Given that the CC was not directly lesioned (as demonstrated by < 0.05% of overlap between the lesion and the CC), the reduction in FA across the CC is evidence for transcallosal diaschisis.

Lower FA specifically in the non-primary sensorimotor regions, the prefrontal (CC1) and premotor and supplementary motor regions (CC2), supported our a-priori hypothesis regarding the involvement of non-primary sensorimotor regions. In fact, CC2 showed the second largest magnitude of the effect of stroke, second only to the motor region of CC—a novel finding in this study. Changes observed in CC1 and CC2 are especially interesting as they suggest that transcallosal reorganization after stroke not only impacts the primary motor region, but also constituent regions of the larger sensorimotor networks, involved in the control of complex motor actions that require anticipatory motor planning and sequencing. Reductions in FA in the primary motor and primary somatosensory regions of the CC were less surprising and generally consistent with previous reports, with fairly similar effect sizes (ΔFA ~0.05) to those reported by Stewart, Dewanjee, et al. (2017) in mild-to-moderate chronic stroke survivors.

The lack of a group difference in the splenium is also interesting. One straightforward explanation for this finding is that lesions were highly localized to the primary motor areas and the descending motor pathways, thus impacting the body of the CC. In about 9 individuals in our sample, lesions also involved frontal areas, and so could result in microstructural changes along the genu of the CC. However, only about 5 of the 41 stroke survivors had any involvement of the temporal or parietal cortex, and none had damage to the occipital cortex, thus sparing the splenium. A related factor that complicates the interpretation of this finding is that the splenium comprises of heterogeneous fiber populations connecting the parietal, temporal and occipital regions. For this reason, unlike other regions of the CC, directional orientation of fibers are not easily disambiguated and might make potential group differences in any one region less detectable. Techniques to geometrically segment the splenium to delineate the different fiber populations have been developed and implemented in adults without brain lesions. However, because these techniques rely on probabilistic

tractography, they might render unreliable results in those with stroke due to lesion-induced tissue loss.

4.3. The effect of age and regional differences in CC

Although not central to this study, we also found a strong and expected effect of age and an effect of CC region, in a pattern consistent with previously reported topographical organization of the CC.

First, an exploration of the effect of age suggests that aging explained ~19% of the unadjusted variance in mean FA across the CC (Supplementary Material IV). In our secondary analysis where we modeled age as a categorical variable, we noted that stroke survivors were approximately 8 years younger than the older controls, which could hypothetically lend an age-related advantage to stroke survivors. This was not the case; in fact, stroke seemed to exacerbate the effect of aging in all regions of the CC where a significant group effect was observed. This is evidenced by most of the data points for stroke survivors lying below the least-squares line in the plot (Supplementary Material IV). It also appears that the largest magnitude of the effect of age in the control group was observed for the prefrontal region, aligning well with previously reported structural changes in the gray and white matter in the frontal lobe and associations with age-related decline in executive function, decision making, and movement planning (e.g., Voineskos et al., 2012).

Second, in all three groups, across the 5 regions, we observed a specific pattern in that FA values were largest for the most posterior regions of the CC (the splenium), followed by the most anterior regions (the genu) and were smallest in the midbody. This is consistent with the cytoarchitectonic properties (e.g., fiber density, size, and myelination) observed through microscopic examination of the various regions of CC and validates the composite FA metric as bearing good correspondence with such properties (Basser & Pierpaoli, 2011).

4.4. Contributions of other metrics of structural damage

We intended to focus all our planned analyses on the corpus callosum. However, the callosal account of reorganization after stroke is only a partial one. As noted earlier, stroke-related transcallosal changes occur as a result of a dual process: metabolic and degenerative changes in the ipsilesional cortex and secondary reorganization in the contralesional cortex. Whatever the changes in either hemisphere, the main assumption in this study is that the evolving dynamics of interhemispheric relationship would manifest within the microstructure of the primary commissure.

Taking into consideration the first of these processes, we included metrics of ipsilesional structural damage in our regression model and found three measures to be of significant additive value in explaining bimanual performance: the integrity of white matter directly underlying the lesion (lesion FA), the relative enlargement of the ipsilesional to the contralesional ventricle, and the direct injury to the corticospinal tract. The latter two have been previously shown to be important predictors of unimanual motor outcomes.

4.5. Limitations and Future Directions

The use of control datasets acquired on a different scanner raises the issue of scanner-related variability. It is possible that unknown differences in proprietary scanner technology may have confounded observed group differences. Several attempts were made to address this issue: first, the control dataset was comparable to our stroke data in terms of critical diffusion imaging acquisition parameters (e.g., diffusion intensity, 1000s/mm2, directions, 64). Second,

to offset random variances by estimating scanner-related random effects in the mixed model. Finally, for all 3 groups, we were able to reproduce expected regional differences in FA values across the CC, and a range of FA values, especially in the sensorimotor CC, similar to those reported in previous studies. This provides methodological validity to our data.

Known limitations of diffusion tensor fitting include interpretation of isotropic FA values as poor directional orientation in voxels where multiple fiber populations intersect. This issue is particularly pronounced with long distance projections, such as the corticospinal tracts, and is at least in part bypassed by homogenous and homotopic fibers of the CC. Another limitation is that we selected a very small subset of bimanual tasks—folding and inserting the letter—of a known large repertoire of bimanual skills. We chose this task because we had previously found it to be most likely to elicit a bimanual strategy (Varghese et al., 2020). The task also presented with the opportunity to study naturalistic real-world performance in which participants are self-guided and self-paced. However, to be able to generalize these findings, follow up studies are needed.

Complementary structural changes in the contralesional cortex may also be important but were not assessed in this study. The extant role of the contralesional cortex is a matter of much debate. Some suggest that the progressive involvement of compensatory tracts (e.g., cortico-reticulospinal pathways) in the contralesional cortex through substitutionary use of the less-affected arm, is maladaptive and may be detrimental toward behavioral restitution and recovery of ipsilesional pathways. Others propose that such maladaptive changes do not emerge until later after the stroke (Cirillo et al., 2020; Xu et al., 2019), and that secondary motor areas in the contralesional cortex play an important role in the performance of complex motor tasks after stroke (Hoyer & Celnik, 2011; Lotze et al., 2006) and must therefore be engaged. Future studies could characterize the likely time- and task-dependent changes in contralesional white matter to clarify its role in post-stroke recovery.

Finally, retrospective design and a relatively modest sample size are also issues. Whereas correlational analysis is the current standard in research using structural imaging for brain-behavior analysis, future work that extends structural diffusion imaging to multi-modal imaging including functional MRI along with larger samples and a prospective design might reveal new insights into transcallosal diaschisis after stroke in humans.

5. CONCLUSION

Findings of this study lead us to conclude that in mild-to-moderate chronic stroke survivors with relatively localized lesions to the motor areas, callosal microstructure can be expected to change not only in the primary sensorimotor region, but also in the premotor, supplementary motor and prefrontal regions. These remote widespread changes in the callosal genu and body are likely to impact performance on cooperative bimanual tasks that require precise and interdependent coordination of the hands.

Acknowledgements

Tae-Ho Lee (Virginia Tech) and Mara Mather (USC Gerontology) for sharing DTI acquisition parameters and participant age for their OpenNeuro dataset. Members of the Neuroplasticity and Neurorehabilitation laboratory (USC Chan Division of Occupational Science and Occupational Therapy) for helpful discussions.

Funding

This research study is supported by the National Institutes of Health under award numbers:

- NICHD F31HD098796 to RV
- NICHD R01HD065438 to CW and NS
- NINDS R56NS100528 to NS
- NINDS R21NS120274 to NS

Data and code availability

Data table and code for analysis are available in the first author's OSF repository: osf.io/7j9xe

REFERENCES

1. Andersson, J. L. R., Jenkinson, M., & Smith, S. (2007a). Non-linear optimisation. FMRIB technical report TR07JA1. *Practice*.
2. Andersson, J. L. R., Jenkinson, M., & Smith, S. (2007b). Non-linear registration, aka Spatial normalisation FMRIB technical report TR07JA2. *FMRIB Analysis Group of the University of Oxford*, *2*(1), e21.
3. Basser, P. J., & Pierpaoli, C. (2011). Microstructural and physiological features of tissues elucidated by quantitative-diffusion-tensor MRI. *Journal of Magnetic Resonance*, *213*(2), 560–570. https://doi.org/10.1016/j.jmr.2011.09.022
4. Baxter, M. G., Parker, A., Lindner, C. C. C., Izquierdo, A. D., & Murray, E. A. (2000). Control of response selection by reinforcer value requires interaction of amygdala and orbital prefrontal cortex. *Journal of Neuroscience*, *20*(11), 4311–4319. https://doi.org/10.1523/jneurosci.20-11-04311.2000
5. Bonzano, L., Tacchino, A., Roccatagliata, L., Abbruzzese, G., Mancardi, G. L., & Bove, M. (2008). Callosal contributions to simultaneous bimanual finger movements. *Journal of Neuroscience*, *28*(12), 3227–3233. https://doi.org/10.1523/JNEUROSCI.4076-07.2008
6. Brinkman, J., & Kuypers, H. G. J. M. (1973). Cerebral control of contralateral and ipsilateral arm, hand and finger movements in the split-brain rhesus monkey. *Brain*, *96*(4), 653–674. https://doi.org/10.1093/brain/96.4.653
7. Caeyenberghs, K., Leemans, A., Coxon, J., Leunissen, I., Drijkoningen, D., Geurts, M., Gooijers, J., Michiels, K., Sunaert, S., & Swinnen, S. P. (2011). Bimanual coordination and corpus callosum microstructure in young adults with traumatic brain injury: A diffusion tensor imaging study. *Journal of Neurotrauma*, *28*(6), 897–913. https://doi.org/10.1089/neu.2010.1721
8. Cirillo, C., Brihmat, N., Castel-Lacanal, E., Le Friec, A., Barbieux-Guillot, M., Raposo, N., Pariente, J., Viguier, A., Simonetta-Moreau, M., Albucher, J. F., Olivot, J. M., Desmoulin, F., Marque, P., Chollet, F., & Loubinoux, I. (2020). Post-stroke remodeling processes in animal models and humans. *Journal of Cerebral Blood Flow and Metabolism*, *40*(1), 3–22. https://doi.org/10.1177/0271678X19882788
9. Egorova, N., Dhollander, T., Khlif, M. S., Khan, W., Werden, E., & Brodtmann, A. (2020). Pervasive White Matter Fiber Degeneration in Ischemic Stroke. *Stroke*, 1507–1513. https://doi.org/10.1161/STROKEAHA.119.028143
10. Egorova, N., Liem, F., Hachinski, V., & Brodtmann, A. (2019). Predicted Brain Age After Stroke. *Frontiers in Aging Neuroscience*, *11*(December), 4–11. https://doi.org/10.3389/fnagi.2019.00348
11. Eliassen, J. C., Baynes, K., & Gazzaniga, M. S. (2000). Anterior and posterior callosal contributions to simultaneous bimanual movements of the hands and fingers. *Brain*, *123*(12), 2501–2511. https://doi.org/10.1093/brain/123.12.2501
12. Findlater, S. E., Mazerolle, E. L., Pike, G. B., & Dukelow, S. P. (2019). Proprioception and motor performance after stroke: An examination of diffusion properties in sensory and motor pathways. *Human Brain Mapping*, *40*(10), 2995–3009.
13. Fling, B. W., & Seidler, R. D. (2012). Fundamental differences in callosal structure, neurophysiologic function, and bimanual control in young and older adults. *Cerebral Cortex*, *22*(11), 2643–2652. https://doi.org/10.1093/cercor/bhr349
14. Fling, Brett W., Walsh, C. M., Bangert, A. S., Reuter-Lorenz, P. A., Welsh, R. C., & Seidler, R. D. (2011). Differential callosal contributions to bimanual control in young and older adults. *Journal of Cognitive Neuroscience*, *23*(9), 2171–2185. https://doi.org/10.1162/jocn.2010.21600
15. Franz, E. A., Eliassen, J. C., Ivry, R. B., & Gazzaniga, M. S. (1996). Dissociation of Spatial and Temporal Coupling in the Bimanual Movements of Callosotomy Patients. *Psychological Science*, *7*(5), 306–310. https://doi.org/10.1111/j.1467-9280.1996.tb00379.x
16. Gooijers, J., Caeyenberghs, K., Sisti, H. M., Geurts, M., Heitger, M. H., Leemans, A., & Swinnen, S.

P. (2013). Diffusion tensor imaging metrics of the corpus callosum in relation to bimanual coordination: Effect of task complexity and sensory feedback. *Human Brain Mapping*, *34*(1), 241–252. https://doi.org/10.1002/hbm.21429

17. Gratton, C., Nomura, E. M., Pérez, F., & D'Esposito, M. (2012). Focal brain lesions to critical locations cause widespread disruption of the modular organization of the brain. *Journal of Cognitive Neuroscience*, *24*(6), 1275–1285.
18. Hagmann, P., Jonasson, L., Maeder, P., Thiran, J.-P., Wedeen, V. J., & Meuli, R. (2006). Understanding Diffusion MR Imaging Techniques : From Scalar Imaging to Diffusion. *Radiographics*, *26*, 205–224.
19. Halsband, U., Ito, N., Tanji, J., & Freund, H.-J. (1993). The role of premotor cortex and the supplementary motor area in the temporal control of movement in man. *Brain*, *116*(1), 243–266.
20. Hawe, R. L., Sukal-Moulton, T., & Dewald, J. P. A. (2013). The effect of injury timing on white matter changes in the corpus callosum following unilateral brain injury. *NeuroImage: Clinical*, *3*, 115–122. https://doi.org/10.1016/j.nicl.2013.08.002
21. Hayward, K. S., Neva, J. L., Mang, C. S., Peters, S., Wadden, K. P., Ferris, J. K., & Boyd, L. A. (2017). Interhemispheric Pathways Are Important for Motor Outcome in Individuals with Chronic and Severe Upper Limb Impairment Post Stroke. *Neural Plasticity*, *2017*. https://doi.org/10.1155/2017/4281532
22. Hofer, S., & Frahm, J. (2006). Topography of the human corpus callosum revisited-Comprehensive fiber tractography using diffusion tensor magnetic resonance imaging. *NeuroImage*, *32*(3), 989–994. https://doi.org/10.1016/j.neuroimage.2006.05.044
23. Hoyer, E. H., & Celnik, P. A. (2011). Understanding and enhancing motor recovery after stroke using transcranial magnetic stimulation. *Restorative Neurology and Neuroscience*, *29*(6), 395–409.
24. Jenkinson, M., Beckmann, C. F., Behrens, T. E. J., Woolrich, M. W., & Smith, S. M. (2012). Fsl. *Neuroimage*, *62*(2), 782–790.
25. Jenkinson, M., Pechaud, M., & Smith, S. (2005). BET2: MR-based estimation of brain, skull and scalp surfaces. *Eleventh Annual Meeting of the Organization for Human Brain Mapping*, *17*, 167.
26. Jones, T. A., & Adkins, D. L. (2015). Motor system reorganization after stroke: Stimulating and training toward perfection. *Physiology*, *30*(5), 358–370. https://doi.org/10.1152/physiol.00014.2015
27. Jones, T. A., & Schallert, T. (1992). Overgrowth and pruning of dendrites in adult rats recovering from neocortical damage. *Brain Research*, *581*(1), 156–160. https://doi.org/10.1016/0006-8993(92)90356-E
28. Jones, T. A., & Schallert, T. (1994). Use-dependent growth of pyramidal neurons after neocortical damage. *Journal of Neuroscience*, *14*(4), 2140–2152.
29. Kazennikov, O., Hyland, B., Wicki, U., Perrig, S., Rouiller, E. M., & Wiesendanger, M. (1998). Effects of lesions in the mesial frontal cortex on bimanual co- ordination in monkeys. *Neuroscience*, *85*(3), 703–716. https://doi.org/10.1016/S0306-4522(97)00693-3
30. Kim, B. (2017). Relationship Between Brain Structure and Motor Behavior in Chronic Stroke Survivors [University of Southern California]. In *ProQuest Dissertations and Theses*. http://libproxy.usc.edu/login?url=https://www.proquest.com/dissertations-theses/relationship-between-brain-structure-motor/docview/2157894775/se-2?accountid=14749
31. Kim, B., & Winstein, C. (2017). Can Neurological Biomarkers of Brain Impairment Be Used to Predict Poststroke Motor Recovery? A Systematic Review. *Neurorehabilitation and Neural Repair*, *31*(1), 3–24. https://doi.org/10.1177/1545968316662708
32. Kornysheva, K., & Diedrichsen, J. (2014). Human premotor areas parse sequences into their spatial and temporal features. *Elife*, *3*, e03043.
33. Krakauer, J. W., & Carmichael, S. T. (2017). *Broken movement : the neurobiology of motor recovery after stroke*. MIT Press. https://books.google.fr/books?hl=en&lr=&id=Mpg-DwAAQBAJ&oi=fnd&pg=PR7&dq=broke+movements+krakauer&ots=Wm1RH20iah&sig=7GcgC_eEMYvyRCH5r84XjxV1grk#v=onepage&q&f=false

34. Li, Y., Wu, P., Liang, F., & Huang, W. (2015). The microstructural status of the corpus callosum is associated with the degree of motor function and neurological deficit in stroke patients. *PLoS ONE*, *10*(4), 1–17. https://doi.org/10.1371/journal.pone.0122615
35. Liew, S. L., Anglin, J. M., Banks, N. W., Sondag, M., Ito, K. L., Kim, H., Chan, J., Ito, J., Jung, C., Khoshab, N., Lefebvre, S., Nakamura, W., Saldana, D., Schmiesing, A., Tran, C., Vo, D., Ard, T., Heydari, P., Kim, B., … Stroud, A. (2017). A large, open source dataset of stroke anatomical brain images and manual lesion segmentations. *BioRxiv*, 1–11. https://doi.org/10.1101/179614
36. Lindenberg, R., Zhu, L. L., Rüber, T., & Schlaug, G. (2012). Predicting functional motor potential in chronic stroke patients using diffusion tensor imaging. *Human Brain Mapping*, *33*(5), 1040–1051. https://doi.org/10.1002/hbm.21266
37. Lotze, M., Markert, J., Sauseng, P., Hoppe, J., Plewnia, C., & Gerloff, C. (2006). The role of multiple contralesional motor areas for complex hand movements after internal capsular lesion. *Journal of Neuroscience*, *26*(22), 6096–6102. https://doi.org/10.1523/JNEUROSCI.4564-05.2006
38. Pierpaoli, C., & Basser, P. J. (1996). Toward a quantitative assessment of diffusion anisotropy. *Magnetic Resonance in Medicine*, *36*(6), 893–906. https://doi.org/10.1002/mrm.1910360612
39. Pinter, D., Gattringer, T., Fandler-Höfler, S., Kneihsl, M., Eppinger, S., Deutschmann, H., Pichler, A., Poltrum, B., Reishofer, G., Ropele, S., Schmidt, R., & Enzinger, C. (2020). Early Progressive Changes in White Matter Integrity Are Associated with Stroke Recovery. *Translational Stroke Research*, *11*(6), 1264–1272. https://doi.org/10.1007/s12975-020-00797-x
40. Preilowski, B. F. B. (1972). Possible contribution of the anterior forebrain commissures to bilateral motor coordination. *Neuropsychologia*, *10*(3), 267–277. https://doi.org/10.1016/0028-3932(72)90018-8
41. Puig, J., Blasco, G., Schlaug, G., Stinear, C. M., Daunis-i-Estadella, P., Biarnes, C., Figueras, J., Serena, J., Hernández-Pérez, M., Alberich-Bayarri, A., Castellanos, M., Liebeskind, D. S., Demchuk, A. M., Menon, B. K., Thomalla, G., Nael, K., Wintermark, M., & Pedraza, S. (2017). Diffusion tensor imaging as a prognostic biomarker for motor recovery and rehabilitation after stroke. *Neuroradiology*, *59*(4), 343–351. https://doi.org/10.1007/s00234-017-1816-0
42. Rorden, C., & Brett, M. (2000). Lesion analysis. *Behavioural Neurology*, *12*(0953–4180), 191–200. www.fil.ion.ucl.ac.uk/spm/
43. Rowe, J. B., Toni, I., Josephs, O., Frackowiak, R. S. J., & Passingham, R. E. (2000). The prefrontal cortex: Response selection or maintenance within working memory? *Science*, *288*(5471), 1656–1660. https://doi.org/10.1126/science.288.5471.1656
44. Rueckert, D., Sonoda, L. I., Hayes, C., Hill, D. L. G., Leach, M. O., & Hawkes, D. J. (1999). Nonrigid registration using free-form deformations: application to breast MR images. *IEEE Transactions on Medical Imaging*, *18*(8), 712–721.
45. Sadato, N., Yonekura, Y., Waki, A., Yamada, H., & Ishii, Y. (1997). Role of the supplementary motor area and the right premotor cortex in the coordination of bimanual finger movements. *Journal of Neuroscience*, *17*(24), 9667–9674.
46. Sisti, H. M., Geurts, M., Gooijers, J., Heitger, M. H., Caeyenberghs, K., Beets, I. A. M., Serbruyns, L., Leemans, A., & Swinnen, S. P. (2012). Microstructural organization of corpus callosum projections to prefrontal cortex predicts bimanual motor learning. *Learning and Memory*, *19*(8), 351–357. https://doi.org/10.1101/lm.026534.112
47. Smith, S. M. (2002). Fast robust automated brain extraction. *Human Brain Mapping*, *17*(3), 143–155. https://doi.org/10.1002/hbm.10062
48. Smith, S. M., Jenkinson, M., Johansen-Berg, H., Rueckert, D., Nichols, T. E., Mackay, C. E., Watkins, K. E., Ciccarelli, O., Cader, M. Z., & Matthews, P. M. (2006). Tract-based spatial statistics: voxelwise analysis of multi-subject diffusion data. *Neuroimage*, *31*(4), 1487–1505.
49. Smith, S. M., Jenkinson, M., Woolrich, M. W., Beckmann, C. F., Behrens, T. E. J., Johansen-Berg, H., Bannister, P. R., De Luca, M., Drobnjak, I., Flitney, D. E., Niazy, R. K., Saunders, J., Vickers, J., Zhang, Y., De Stefano, N., Brady, J. M., & Matthews, P. M. (2004). Advances in functional and

structural MR image analysis and implementation as FSL. *NeuroImage*, *23*(SUPPL. 1), S208–S219. https://doi.org/10.1016/j.neuroimage.2004.07.051

50. Soares, J. M., Marques, P., Alves, V., & Sousa, N. (2013). A hitchhiker's guide to diffusion tensor imaging. *Frontiers in Neuroscience*, *7*(March), 1–14. https://doi.org/10.3389/fnins.2013.00031
51. Stephan, K. M., Binkofski, F., Halsband, U., Dohle, C., Wunderlich, G., Schnitzler, A., Tass, P., Posse, S., Herzog, H., Sturm, V., Zilles, K., Seitz, R. J., & Freund, H. J. (1999). The role of ventral medial wall motor areas in bimanual co-ordination. A combined lesion and activation study. *Brain*, *122*(2), 351–368. https://doi.org/10.1093/brain/122.2.351
52. Stewart, J. C., Dewanjee, P., Tran, G., Quinlan, E. B., Dodakian, L., McKenzie, A., See, J., & Cramer, S. C. (2017). Role of corpus callosum integrity in arm function differs based on motor severity after stroke. *NeuroImage: Clinical*, *14*, 641–647. https://doi.org/10.1016/j.nicl.2017.02.023
53. Stewart, J. C., O'Donnell, M., Handlery, K., & Winstein, C. J. (2017). Skilled Reach Performance Correlates with Corpus Callosum Structural Integrity in Individuals with Mild Motor Impairment after Stroke: A Preliminary Investigation. *Neurorehabilitation and Neural Repair*, *31*(7), 657–665. https://doi.org/10.1177/1545968317712467
54. Varghese, R., Kutch, J. J., Schweighofer, N., & Winstein, C. J. (2020). The probability of choosing both hands depends on an interaction between motor capacity and limb-specific control in chronic stroke. *Experimental Brain Research*, *238*, 2569–2579. https://doi.org/10.1007/s00221-020-05909-5
55. Voineskos, A. N., Rajji, T. K., Lobaugh, N. J., Miranda, D., Shenton, M. E., Kennedy, J. L., Pollock, B. G., & Mulsant, B. H. (2012). Age-related decline in white matter tract integrity and cognitive performance: A DTI tractography and structural equation modeling study. *Neurobiology of Aging*, *33*(1), 21–34. https://doi.org/10.1016/j.neurobiolaging.2010.02.009
56. von Monakow, C. (1914). Die Lokalisation im Grosshirn und der Abbau der Funktion durch Kortikale Herde. In *Journal of the American Medical Association: Vol. LXIII* (Issue 9). JF Bergmann. https://doi.org/10.1001/jama.1914.02570090083033
57. Wang, L. E., Tittgemeyer, M., Imperati, D., Diekhoff, S., Ameli, M., Fink, G. R., & Grefkes, C. (2012). Degeneration of corpus callosum and recovery of motor function after stroke: A multimodal magnetic resonance imaging study. *Human Brain Mapping*, *33*(12), 2941–2956. https://doi.org/10.1002/hbm.21417
58. Winstein, C., Kim, B., Kim, S., Martinez, C., & Schweighofer, N. (2019). Dosage Matters: A Phase IIb Randomized Controlled Trial of Motor Therapy in the Chronic Phase after Stroke. *Stroke*, *50*(7), 1831–1837. https://doi.org/10.1161/STROKEAHA.118.023603
59. Xu, J., Branscheidt, M., Schambra, H., Steiner, L., Widmer, M., Diedrichsen, J., Goldsmith, J., Lindquist, M., Kitago, T., Luft, A. R., Krakauer, J. W., Celnik, P. A., Kim, N., Harran, M. D., Hertler, B., & Cortes, J. C. (2019). Rethinking interhemispheric imbalance as a target for stroke neurorehabilitation. *Annals of Neurology*, *85*(4), 502–513. https://doi.org/10.1002/ana.25452
60. Yeh, F. C., Tang, P. F., & Tseng, W. Y. I. (2013). Diffusion MRI connectometry automatically reveals affected fiber pathways in individuals with chronic stroke. *NeuroImage: Clinical*, *2*(1), 912–921. https://doi.org/10.1016/j.nicl.2013.06.014

SUPPLEMENTARY MATERIAL

I. Comparison of DTI acquisition parameters across the groups.

	Control (n = 52)	**Stroke (n = 41)**
Acquired	2016 – 2018	2012 – 2015
Released	2018	2017
MR scanner	Siemens 3T Trio	GE Signa Excite 3T
Sequence	EPI	Spin-echo EPI (single shot)
TR/TE (ms)	10,000/98	10,000/88
FOV (mm)	256 x 256 x 120	256 x 256 x 132
Matrix Dimensions	128 x 128 x 60	128 x 128
Slices	96	59
Voxel Size	2 x 2 x 2	1 x 1 x 2
b-values (s/mm^2)	1000	1000
# of directions	64	64
DOI	10.18112/openneuro.ds001242.v1.0.0	TBD

II. Comparison of mean FA between native and standard space.

There was no difference in mean FA between native and standard space (n = 20). **A.** Subject-wise comparisons of mean FA (t = 0.04, p = 0.97). Mean and confidence intervals of difference in FA between native and standard space after 1000 iterations of bootstrapping is 0.00045 (-0.021, 0.022). **B.** QQ plots of bootstrapped t-statistic plotted against theoretical t-distribution. Mean and confidence intervals of t-statistic after bootstrapping is 0.053 (-1.93, 2.04). **C.** Bootstrapped *t* overlaps with a theoretical *t* distribution which centers on 0. C. Note that for this comparison, mean of all voxels in the standard space were used (not just those included after TBSS thresholding).

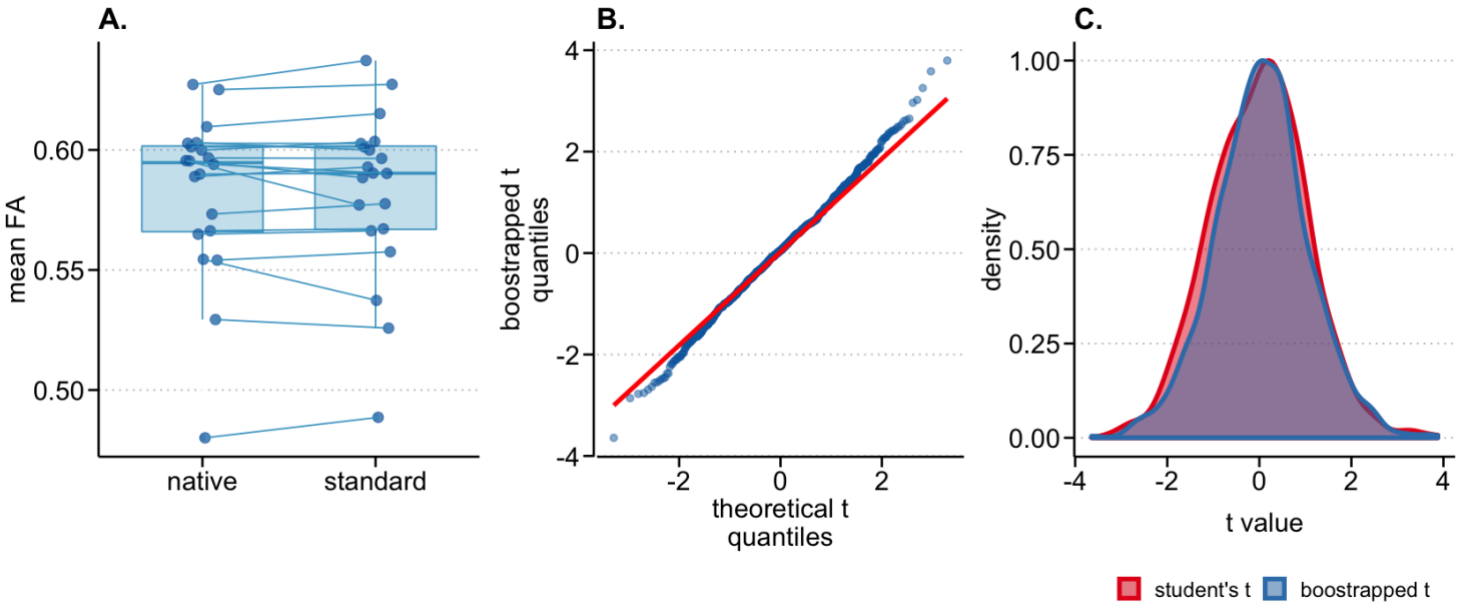

III. Detailed lesion description for all stroke survivors, and availability of bimanual MT and other structural metrics.

ID	Side of Lesion	Vascular Territory	Location	Volume (cm^3)	Bimanual MT available? *	Other structural metrics available?
dose_2001	Right	MCA	Frontal lobe	112.244	✓	✓
dose_2002	Right	MCA	Frontal, Temporal lobes	120.72	-	-
dose_2003	Right	Lacunar	Corona radiata	0.821	✓	✓
dose_2004	Left	ACA/MCA	Frontal, parietal lobe	29.763	✓	✓
dose_2005	Left	Lacunar	Lentiform nucleus, corona radiata	31.417	✓	✓
dose_2006	Right	Basilar perforator	Right hemipons	0.228	-	-
dose_2007	Right	Lacunar	Lentiform nucleus, corona radiata	4.206	✓	✓
dose_2008	Left	Basilar perforator	Left hemipons	0.703	-	-
dose_2009	Right	MCA	Pre- and post-central gyri	8.572	✓	✓
dose_2010	Right	MCA	Frontal, parietal, temporal lobes, basal ganglia	107.05	-	-
dose_2011	Right	MCA	Frontal lobe	14.456	✓	✓
dose_2012	Left	Lacunar	Basal ganglia, corona radiata	13.32	✓	-
dose_2013	Left	MCA	Frontal lobe (precentral gyrus)	6.049	✓	✓
dose_2014	Left	Lacunar	Basal ganglia, corona radiata	15.78	✓	✓
dose_2015	Left	Lacunar	Basal ganglia, corona radiata	6.4	✓	✓
dose_2016	Left	Lacunar	Basal ganglia, thalmus	5.94	✓	✓
dose_2017	Left	Basilar perforator	Right hemipons	0.339	-	-
dose_2018	Right	Lacunar	Basal ganglia	0.267	✓	✓
dose_2019	Right	MCA	Frontal lobe, basal ganglia	78.512	✓	✓
dose_2020	Right	MCA	Temporal operculum, insular cortex	72.996	✓	✓
dose_2021	Right	MCA	Frontal lobe, basal ganglia	2.002	✓	✓
dose_2022	Right	Lacunar	Corona radiata, basal ganglia	55.786	✓	✓
dose_2023	Left	Lacunar	Basal ganglia	0.016	✓	✓
dose_2024	Right	Basilar perforator	Cerebral peduncle	1.01	-	-
dose_2025	Right	Lacunar	Corona radiata, basal ganglia	4.575	✓	✓
dose_2026	Left	Lacunar	Corona radiata, basal ganglia	3.245	✓	✓
dose_2027	Left	Lacunar	Corona radiata, basal ganglia	1.289	✓	✓
dose_2028	Right	Lacunar	Basal ganglia	0.14	✓	✓
dose_2029	Left	Lacunar	Corona radiata	2.448	✓	✓
dose_2030	Left	Basilar perforator	Right hemipons	6.526	✓	✓
dose_2031	Left	Lacunar	Corona radiata, basal ganglia	37.352	✓	-
dose_2032	Left	Lenticulostriate	Basal ganglia, internal capsule	5.799	✓	✓
dose_2033	Left	Lacunar	Thalamus	33.029	✓	✓
dose_2034	Left	MCA	Frontal lobe	3.495	✓	✓
dose_2035	Left	Lacunar	Basal ganglia	6.54	-	-
dose_2036	Left	MCA	Corona radiata, basal ganglia	23.324	✓	✓
dose_2037	Left	PCA/upper branch of the SCA	Right anterior lobe of the cerebellum, posterior and inferior temporal gyrus	5.085	✓	✓
dose_2038	Right	Lacunar	Corona radiata	6.145	-	-
dose_2039	Right	Lacunar	Basal ganglia	4.524	-	-
dose_2040	Right	Lacunar	Thalamus	3.425	-	-
dose_2041	Left	MCA	Pre- and post-central gyri, posterior parietal	26.205	✓	✓

* chose a bimanual strategy for atleast one of the two components

IV. Relationship between age and mean FA.

A simple unadjusted correlation and linear regression was done post-hoc to explore the effects of age on mean FA across the 93 participants. The regression equation displayed on the plot below shows that from an average FA value of 0.81 across participants, mean FA decreases by a factor of 0.00095 for every year. As can be seen in this plot, most of the data points for stroke survivors lying below the least-squares line.

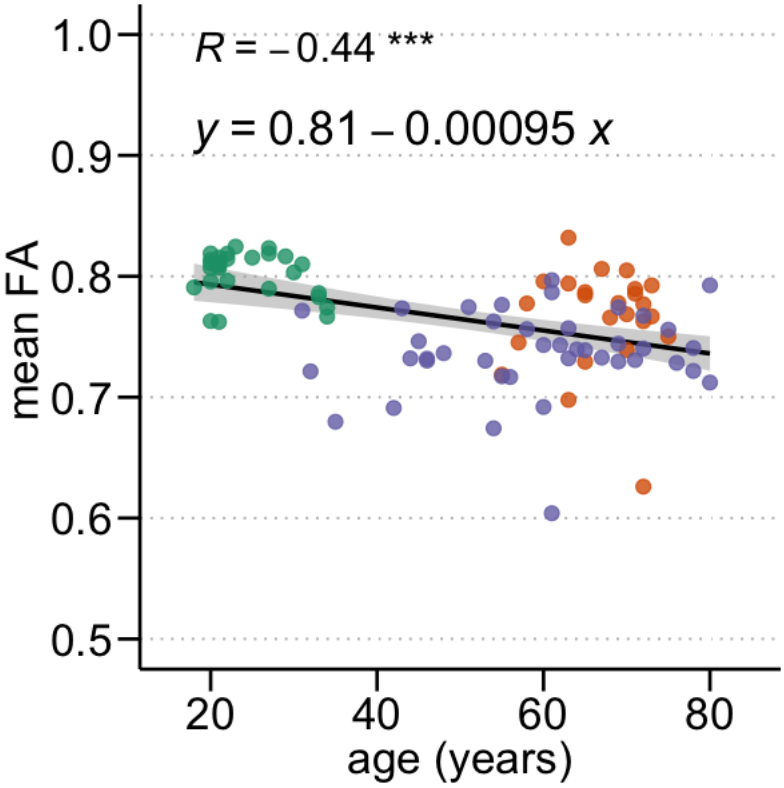

V. Additive value of other metrics of structural damage to predict bimanual performance. Left-hand column is model without other structural damage metrics and right-hand column is the model with these metrics.

	log(mt)			log(mt)		
Predictors	*Estimates*	*CI*	*p*	*Estimates*	*CI*	*p*
(Intercept)	5.59	4.49 – 6.69	**<0.001**	6.20	5.31 – 7.09	**<0.001**
Mean FA	-4.01	-5.72 – -2.30	**<0.001**	-4.52	-5.92 – -3.11	**<0.001**
log(Chronicity)	0.15	0.07 – 0.24	**<0.001**	0.17	0.10 – 0.24	**<0.001**
Total Norm. CC Volume	-0.19	-0.33 – -0.04	**0.011**	-0.23	-0.36 – -0.11	**<0.001**
FA: CC1	0.36	-0.01 – 0.73	0.057	0.41	0.11 – 0.71	**0.007**
FA: CC2	0.16	-0.20 – 0.51	0.386	0.18	-0.10 – 0.47	0.207
FA: CC4	0.43	0.05 – 0.81	**0.025**	0.49	0.18 – 0.80	**0.002**
FA: CC5	0.78	0.33 – 1.24	**0.001**	0.89	0.51 – 1.26	**<0.001**
Lat. Ventr. AI				0.72	0.32 – 1.12	**<0.001**
CST Lesion Load				0.01	-0.00 – 0.02	0.090
Lesion FA				-1.72	-2.60 – -0.85	**<0.001**
Random Effects						
σ^2	0.17			0.13		
τ_{00}	$0.11_{\text{CC\_region:subjID}}$			$0.05_{\text{CC\_region:subjID}}$		
ICC	0.39			0.28		
N	$5_{\text{CC\_region}}$			$5_{\text{CC\_region}}$		
	31_{subjID}			29_{subjID}		
Observations	270			260		
Marginal R^2 / Conditional R^2	0.204 / 0.514			0.373 / 0.546		

As seen above, lateral ventricular volume asymmetry (Lat. Ventr. AI) and Lesion FA provided statistically significant additive value to CC metrics alone in explaining bimanual performance.